Structural Investigations of Calcium Binding Molecules. III. The Calcium–Oxydiacetic Acid System. Crystal and Molecular Structures of Calcium Oxydiacetate Hexahydrate and Raman Spectroscopic Comparison with Species in Aqueous Solution[1]

Vernon A. Uchtman* and Richard P. Oertel

Contribution from the Miami Valley Laboratories, The Procter & Gamble Company, Cincinnati, Ohio 45239. *Received August 30, 1972*

Abstract: A combination of single-crystal X-ray diffraction and Raman spectroscopic techniques has been used to structurally characterize the complexation between Ca^{2+} and species of oxydiacetic acid, $O(CH_2CO_2H)_2$. The crystal and molecular structures of calcium oxydiacetate (ODA) hexahydrate were determined by three-dimensional X-ray crystal structure analysis using the symbolic addition procedure. $CaODA \cdot 6H_2O$ crystallizes in monoclinic space group $P2_1/a$ with $a = 12.830 \pm 0.004$ Å, $b = 15.915 \pm 0.005$ Å, $c = 6.185 \pm 0.002$ Å, $\beta = 118.03 \pm 0.05°$, and four formula units per unit cell. Full-matrix least-squares refinement using automated diffractometer-collected data resulted in $R_1 = 6.1\%$ and $R_2 = 3.9\%$. The crystal structure consists of $CaODA \cdot 5H_2O$ complexes linked only by hydrogen bonding involving the sixth water molecule. The Ca^{2+} coordination is eightfold, consisting of oxygen atoms from five water molecules and two carboxylate groups and the ether oxygen of the tridentate ODA ligand. The CCOCC framework of the ligand is in the trans–trans conformation; with respect to all carbon and oxygen atoms the ligand is nearly planar and the Ca^{2+} ion lies in this plane as part of two adjacent five-membered chelate rings. Raman spectra of this solid and of an aqueous solution containing CaODA(aq) are remarkably similar; it is concluded that the ODA skeletal conformations are identical (trans–trans) in both solution and solid complexed states. The spectrum obtained for an ODA solution not containing a strongly complexing metal ion such as Ca^{2+} is best explained as arising from a mixture of rotational isomers. Addition of Ca^{2+} to such a solution results in extensive spectral changes due to conformational interconversion of ODA to the trans–trans form upon complexation. Spectral assignments are presented which substantiate these conclusions. Possible biological implications of the trans–trans chelate structure induced by Ca^{2+} complexation are discussed. Additional Raman spectroscopic evidence was found for binding between Ca^{2+} and neutral oxydiacetic acid (H_2ODA); this complexation, although weak, is sufficient to result in conformational changes similar to those found upon formation of CaODA. Quantitative measurement of Raman intensities led to the concentration formation quotient $K_{CaH_2ODA^{2+}} = 0.56 \pm 0.15\ M^{-1}$ at *ca.* 30°.

A sound understanding of Ca^{2+} binding and sequestration at the molecular level is critical to the meaningful interpretation and control of the many biological functions and biochemical reactions which have a dependence on Ca^{2+}. As part of a program to investigate the molecular structural characteristics of Ca^{2+} binding, we undertook an examination of Ca^{2+} complexation with oxydiacetic acid, $O(CH_2CO_2H)_2$ (H_2ODA).[2] Calcium binding with a relatively simple organic molecule such as H_2ODA can serve as a useful model for Ca^{2+} interactions with biologically important molecules.

The binding of Ca^{2+} to ether oxygen is of particular interest in view of recent evidence for interaction between metal ions (particularly alkali metal ions) and ether oxygens in macrocyclic antibiotics and cyclic polyether "crown" compounds.[3] Previous studies of aqueous complex formation constants have suggested a significant interaction between the ether oxygen atom of the ODA dianion and Ca^{2+}; log K_1 for the CaODA complex is reported to be 3.4,[4] compared to 2.7 for calcium iminodiacetate[4] and 1.1 for calcium glutarate,[5] the nitrogen and carbon analogs, respectively.

In order to assess the structural implications of this interaction, as well as structurally characterize Ca^{2+}–ODA binding in general, we carried out a single-crystal X-ray analysis of $CaODA \cdot 6H_2O$ and used Raman spectroscopy to relate the structure in the solid state to that in aqueous solution. Raman spectroscopy is an effective technique for making a detailed comparison of this sort, since complete spectra can easily be recorded for both solid and aqueous phases and depolarization data can aid in formulating vibrational assignments for solution species. Infrared spectroscopy, though useful, has shortcomings in both these regards. By use of this combination of X-ray and Raman techniques we have been able to determine without a reasonable doubt the molecular structure of the CaODA complex in both solid and aqueous solution states. At the same time we have observed the considerable effect that Ca^{2+} binding induces on the molecular conformation of this model ligand in aqueous solution. Additional Raman spectroscopic studies have revealed measurable complexation between Ca^{2+} and neutral H_2ODA in aqueous solution.

Experimental Section

Preparation of $CaODA \cdot 6H_2O$. Crystals of $CaODA \cdot 6H_2O$ suit-

(1) (a) Previous paper in this series: V. A. Uchtman, *J. Phys. Chem.*, 76, 1304 (1972); (b) presented in part at the XIVth International Conference on Coordination Chemistry, Toronto, Canada, June 22–28, 1972.

(2) Notation to be used is as follows: oxydiacetic acid, H_2ODA; oxydiacetate half-neutralized anion, HODA; oxydiacetate dianion, ODA.

(3) M. R. Truter and C. J. Pedersen, *Endeavour*, 30, 142 (1971).

(4) R. M. Tichane and W. E. Bennett, *J. Amer. Chem. Soc.*, 79, 1293 (1957).

(5) R. K. Cannan and A. Kibrick, *ibid.*, 60, 2314 (1938).

able for single-crystal X-ray (and Raman) analysis were obtained by slow evaporation at room temperature of an aqueous solution equimolar in oxydiacetic acid and calcium chloride; the pH of the solution was initially adjusted to 9 using tetramethylammonium hydroxide. The crystalline material was filtered, water washed, and dried in air. The chemicals used were reagent grade.

Anal. Calcd for $C_4H_{16}O_{11}Ca$: C, 17.1; H, 5.7; Ca, 14.3. Found: C, 17.5; H, 5.8; Ca, 14.0.

The elemental composition was substantiated by the crystal structure determination.

X-Ray Data Collection. A parallelepiped-shaped single crystal of $CaODA \cdot 6H_2O$ having dimensions 0.25 × 0.30 × 0.35 (rotation (*b*) axis) mm was mounted with epoxy cement on a thin glass fiber. Preliminary oscillation, Weissenberg, and precession X-ray photographs indicated monoclinic symmetry. The crystal was optically aligned on a Siemens Automated single-crystal diffractometer and 46 diffraction maxima were manually centered. Lattice constants were obtained (at 25°) by least-squares refinement of the measured θ settings of these 46 reflections. These lattice constants were used to generate diffractometer angle settings for all data reflections. The method of data collection was identical with a previously reported procedure.[6] A total of 2321 observed reflections and 917 unobserved reflections (*i.e.*, net intensity less than three times the standard deviation of the background counts) for which $2\theta \leq 60°$ (Mo Kα radiation) was collected from the *hkl* and $\bar{h}kl$ octants. Data reduction was carried out on a local IBM 1800 computer using local computer programs. No absorption or extinction corrections were applied. The linear absorption coefficient (μ) of 5.96 cm^{-1} for Mo Kα radiation results in a $\mu R_{max} \leq 0.18$ for which the change of absorption correction factors with θ is negligible.[7] The effects of absorption result in extremes for the I/I_0 ratio of 0.835 and 0.874. Thus a reflection of measured intensity 1.0 could vary in intensity from 1.198 to 1.144, *i.e.*, a variation of 2.3% about the mean value. The relatively small values of the real and imaginary dispersion corrections for Mo Kα radiation (*i.e.*, $\Delta f' = 0.2$ and $\Delta f'' = 0.4$ for calcium)[8] were assumed not to have any significant effect on this centrosymmetric crystal.[9] The scattering factors used for all atoms except Ca^{2+} were those compiled by Hanson, *et al.*[10] Ca^{2+} scattering factors were obtained from the International Tables.[11]

Unit Cell and Space Group. Lattice constants (25°) and their estimated standard deviations for this crystal of $Ca[O(CH_2CO_2)_2] \cdot 6H_2O$ are a = 12.830 (4) Å, b = 15.915 (5) Å, c = 6.185 (2) Å, and β = 118.03 (5)°; unit cell volume is 1114.7 Å^3. These lattice constants were used in all calculations. The experimental density of 1.68 ± 0.01 g cm^{-3} (determined by flotation in mixtures of tetrachloroethylene and dibromomethane) agrees well with the value of 1.67 calculated on the basis of four formula species per unit cell. The total number of electrons per unit cell, $F(000)$, is 592. Systematic absences of k odd for $\{00k\}$ and h odd for $\{h0l\}$ uniquely define the probable space group as $P2_1/a$ (C_{2h}^5, No. 14). The assignment of this space group was verified by the successful refinement of the structure in this space group. The solution of the structure required the location of one calcium, 11 oxygen, four carbon, and, ideally, 16 hydrogen atoms, corresponding to one formula unit per unit cell. The crystallographically independent atoms were each found from the structural analysis to occupy the general fourfold set of positions: $\pm(x, y, z;\ ^1/_2 + x, ^1/_2 - y, z)$.

Determination of Structure. The X-RAY 67 system of computer programs,[12] modified for use on the Control Data Corp. 6600 computer, was used for the majority of computing operations. DATFIX was used to calculate quasinormalized structure factors (E's); SIGMA2 was used for generation of σ-2 relationships; and phases were determined using PHASE. Approximately 400 reflections for which $E \geq 1.50$ were used for generation of σ-2 relationships. Only signs with a probability level ≥0.98 were accepted. A three-dimensional Fourier synthesis was computed which used the 191 determined phases. The 13 strongest peaks from this E map were used for a difference-Fourier map which utilized all observed data. This map revealed seven new peaks and indicated four of the original peaks to be erroneous. The resulting total of 16 peaks formed a reasonable model for the nonhydrogen atoms of $Ca[O(CH_2CO_2)_2] \cdot 6H_2O$. Three cycles of full-matrix least-squares refinement (which utilized individual isotropic temperature factors) resulted in discrepancy factors of

$$R_1 = [\sum||F_o| - |F_c||/\sum|F_o|] \times 100 = 12.0$$

$$R_2 = [\sum w||F_o| - |F_c||^2/\sum w|F_o|^2]^{1/2} \times 100 = 12.1$$

Refinement was based on minimization of $\Sigma w_i \Delta F_i^2$, and weights were determined according to the relationship $w_i = 1/\sigma_i^2(F_o)$. Two additional cycles of refinement utilizing individual anisotropic temperature factors resulted in the lowering of R_1 and R_2 to 9.7 and 10.3, respectively. A difference Fourier map calculated at this point revealed reasonable positions for the 16 hydrogen atoms. Three additional cycles of least-squares refinement which utilized anisotropic temperature factors for nonhydrogen atoms and isotropic ones for hydrogen atoms (whose parameters were not varied) resulted in final discrepancy factors of R_1 = 6.1 and R_2 = 3.9. There were no positional parameter shifts greater than 0.125 · σ, where σ is the standard deviation of the parameter. A final difference Fourier map contained no unexplainable irregularities. (Peaks significantly above background could be attributed to uncorrected thermal motion or uncertainties in the unrefined hydrogen atom positions.) Final atomic positional and anisotropic thermal parameters are given in Tables I and II, respectively; Table III lists interatomic distances and angles.[13] The thermal

Table I. Final Atomic Positional Parameters with Their Standard Deviations for $Ca[O(CH_2CO_2)_2] \cdot 6H_2O$

	x ($10^5\sigma_x$)	y ($10^5\sigma_y$)	z ($10^5\sigma_z$)
Ca	0.33474 (6)	0.38341 (4)	0.07966 (13)
O1	0.39090 (22)	0.23853 (15)	0.06506 (48)
O2	0.27182 (21)	0.28157 (15)	0.29115 (46)
O3	0.24757 (22)	0.14753 (15)	0.37193 (47)
O4	0.55171 (24)	0.27342 (15)	−0.26256 (49)
O5	0.44897 (20)	0.35780 (13)	−0.14297 (42)
O6	0.40600 (22)	0.00771 (17)	0.62859 (47)
O7	0.37320 (21)	0.51996 (14)	−0.02052 (47)
O8	0.54562 (19)	0.38248 (16)	0.40281 (39)
O9	0.18496 (22)	0.34507 (15)	−0.35764 (47)
O10	0.34859 (21)	0.45794 (15)	0.43551 (44)
O11	0.14495 (21)	0.45163 (16)	−0.02819 (46)
C1	0.48904 (30)	0.28691 (22)	−0.16104 (64)
C2	0.46380 (32)	0.21231 (21)	−0.04361 (68)
C3	0.35430 (33)	0.17065 (23)	0.15762 (67)
C4	0.28577 (29)	0.20390 (23)	0.28251 (64)
H1[a]	0.5483	0.1950	0.0900
H2	0.4217	0.1667	−0.1433
H3	0.3100	0.1233	0.0733
H4	0.4433	0.1500	0.3000
H5	0.3717	0.5183	0.4833
H6	0.3683	0.4333	0.5667
H7	0.1350	0.4667	0.0967
H8	0.0733	0.4700	−0.1667
H9	0.3133	0.5500	−0.1533
H10	0.4417	0.5467	0.0867
H11	0.5567	0.3550	0.5400
H12	0.6117	0.3617	0.4133
H13	0.1367	0.3183	−0.3600
H14	0.2117	0.3250	−0.4567
H15	0.3250	0.0467	0.5000
H16	0.3450	−0.0400	0.4867

[a] These hydrogen atom positional parameters were obtained from a difference Fourier map and were not refined. They were given isotropic temperature factors of 5.0.

(6) V. A. Uchtman and R. A. Gloss, *J. Phys. Chem.*, **76**, 1298 (1972).
(7) "International Tables for X-Ray Crystallography," Vol. II, Kynoch Press, Birmingham, England, 1959, p 295.
(8) Reference 7, Vol. III, 1962, p 215.
(9) D. H. Templeton, *Acta Crystallogr.*, **8**, 842 (1955).
(10) H. P. Hanson, F. Herman, J. D. Lea, and S. Skillman, *ibid.*, **17**, 1040 (1964).
(11) Reference 7, Vol. III, 1962, p 201.
(12) J. M. Stewart, Technical Report 67-58, Dec. 1967, Computer Science Center, University of Maryland.

(13) A listing of the observed and calculated structure factors and additional discussion of Raman assignments will appear immediately following these pages in the microfilm edition of this volume of the journal. Single copies may be obtained from the Business Operations Office, Books and Journals Division, American Chemical Society, 1155 Sixteenth Street, N.W., Washington, D. C. 20036, by referring to code number JACS-73-1802. Remit check or money order for $3.00 for photocopy, or $2.00 for microfiche.

Table II. Final Anisotropic Temperature Factors[a] with Their Standard Deviations for $Ca[O(CH_2CO_2)_2]\cdot 6H_2O$

	β_{11} ($10^5\sigma$)	β_{22} ($10^5\sigma$)	β_{33} ($10^5\sigma$)	β_{12} ($10^5\sigma$)	β_{13} ($10^5\sigma$)	β_{23} ($10^5\sigma$)
Ca	0.00334 (5)	0.00125 (13)	0.01675 (24)	0.00003 (4)	0.00510 (10)	0.00020 (9)
O1	0.00775 (28)	0.00176 (11)	0.04052 (124)	0.00038 (14)	0.01474 (52)	0.00133 (30)
O2	0.00553 (24)	0.00190 (11)	0.03187 (114)	−0.00015 (13)	0.00912 (44)	−0.00070 (29)
O3	0.00656 (25)	0.00233 (12)	0.03772 (120)	−0.00039 (14)	0.01124 (47)	0.00158 (30)
O4	0.00844 (27)	0.00328 (13)	0.03440 (114)	0.00143 (17)	0.01485 (50)	0.00299 (33)
O5	0.00515 (23)	0.00169 (71)	0.02937 (108)	−0.00001 (12)	0.00823 (43)	0.00032 (27)
O6	0.00509 (25)	0.00418 (14)	0.03144 (119)	−0.00011 (15)	0.00498 (46)	0.00065 (34)
O7	0.00529 (25)	0.00187 (11)	0.03594 (122)	0.00001 (13)	0.00690 (47)	0.00200 (29)
O8	0.00415 (22)	0.00280 (11)	0.02513 (98)	0.00039 (15)	0.00788 (40)	0.00098 (32)
O9	0.00615 (25)	0.00280 (12)	0.03744 (120)	−0.00010 (14)	0.01002 (47)	−0.00183 (32)
O10	0.00628 (25)	0.00239 (11)	0.02508 (105)	−0.00009 (14)	0.00767 (43)	−0.00053 (29)
O11	0.00450 (23)	0.00333 (13)	0.03289 (122)	0.00098 (14)	0.00632 (44)	−0.00003 (32)
C1	0.00394 (31)	0.00200 (16)	0.01966 (145)	0.00017 (18)	0.00376 (56)	0.00062 (39)
C2	0.00642 (36)	0.00186 (15)	0.02888 (160)	0.00025 (20)	0.01078 (67)	0.00033 (41)
C3	0.00663 (38)	0.00184 (15)	0.03612 (177)	−0.00011 (20)	0.01264 (72)	0.00053 (42)
C4	0.00336 (31)	0.00224 (17)	0.02116 (146)	−0.00052 (18)	0.00515 (56)	0.00007 (39)

[a] Anisotropic temperature factors are expressed as $\exp[-(h^2\beta_{11} + k^2\beta_{22} + l^2\beta_{33} + 2hk\beta_{12} + 2hl\beta_{13} + 2kl\beta_{23})]$.

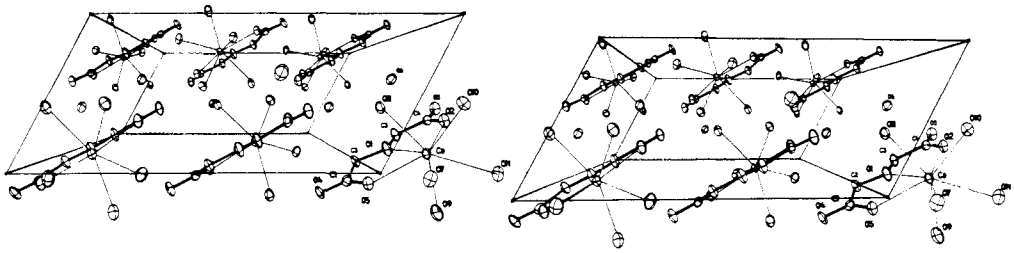

Figure 1. Stereographic crystal packing diagram of $CaODA\cdot 6H_2O$ placed on monoclinic ($P2_1/a$) unit cell axes (positive b axis directed toward viewer). Coordinates of labeled atom positions shown here are related to those in Table I by the following symmetry operation: $1.5 - x, 0.5 + y, 1 - z$.

ellipsoid plot program ORTEP (C. K. Johnson, Oak Ridge National Laboratory) was used for crystal structure illustrations.

Preparation of Samples for Raman Analysis. All chemicals were reagent grade, used without further purification. In general, solutions of known concentration were prepared using standard weighing and volumetric techniques and passed through a Millipore filter prior to spectral recording. Solutions of alkali metal oxydiacetates were made by completely neutralizing H_2ODA with the appropriate hydroxide; the final pH usually was slightly greater than 5 (pK_1 = 2.90, pK_2 = 4.03 at 30°)[4] and there was no evidence of Raman bands due to acid. A solution containing 0.33 M NaHODA was prepared by mixing together solutions containing equimolar amounts of NaOH and H_2ODA. A reasonably stable solution of calcium oxydiacetate (0.18 M in both Ca^{2+} and partially neutralized oxydiacetate species) was prepared by adding aqueous KOH dropwise and with vigorous stirring to a solution containing equimolar H_2ODA and calcium chloride. The acid could only be formally three-fourths neutralized in this manner, as further addition of base caused the solution immediately to cloud. Tetramethylammonium hydroxide was not used here, as it was in the preparation of $CaODA\cdot 6H_2O$ crystals for X-ray analysis, because the tetramethylammonium cation would have contributed interfering Raman bands. The partially neutralized solution, having pH 2.8, slowly deposited crystalline needles, but these did not affect the recording of its Raman spectrum. The spectrum of these crystals was indistinguishable from that of solid $CaODA\cdot 6H_2O$ prepared as described earlier.

Of considerable importance in the present study is knowledge that the $CaODA\cdot 6H_2O$ solid examined by X-ray and Raman methods was one and the same material. The main concern is whether loss of water occurred in the laser beam during the Raman experiment, possibly accompanied by a change in structure of the CaODA complex. We found that when freshly prepared, colorless $CaODA\cdot 6H_2O$ needles were stored in a desiccator for several days or exposed to air for a prolonged period, they became whitened and exhibited Raman bands at, for example, 1059, 1457, and 1628 cm^{-1}. Since there is no evidence of these "dehydration bands" in the spectrum we report for the original material, we regard the possibility that solid $CaODA\cdot 6H_2O$ lost water in the laser beam extremely remote.

Preparation of $Ca(HODA)_2$. From concentrated aqueous solutions containing Ca^{2+} and H_2ODA (pH unadjusted), colorless crystals of $Ca(HODA)_2$ deposited.

Anal. Calcd for $C_8H_{10}O_{10}Ca$: C, 31.4; H, 3.3; Ca, 13.1. Found: C, 31.1; H, 3.3; Ca, 13.4.

The chloride and nitrate salts of calcium yielded crystalline material giving identical Raman spectra, confirming the absence of the inorganic anion. The minimum concentration of calcium salt and H_2ODA tried was 0.25 M, and the molar ratio of Ca^{2+} salt to H_2ODA did not affect the product composition. Both the Raman and infrared (Nujol) spectrum of this compound corroborated the absence of water.

Raman Spectra. Raman spectra were recorded on a Cary 81 spectrophotometer using the 5145-Å line from a Coherent Radiation Laboratories Model 52 Ar^+ laser as excitation source and R136 photomultiplier tubes for detection. The laser power at the sample ranged from 65 to 130 mW, depending on the nature of the sample, and the spectral slit width at 5145 Å was *ca.* 7 cm^{-1} for liquids and *ca.* 5 cm^{-1} for solid samples. The frequency scale was calibrated using indene, CCl_4, and C_6H_6; except for very broad bands and shoulders, positions of band maxima are expected to be accurate to ± 2 cm^{-1}. The 180° excitation-viewing mode was used to obtain spectra of solutions contained in 1.3 mm i.d. Kimax capillaries and ground crystalline samples packed into a conical (Cary) holder. The temperature of solutions in the laser beam was *ca.* 30°.

Depolarization ratios were determined by rotating a half-wave plate in front of the sample and measuring the total scattered radiation (band heights). For these measurements, 2.5-ml samples were contained in a multipass cell held in the 90° illumination-viewing position. A DuPont Model 310 curve resolver aided in resolving overlapping bands for intensity and depolarization measurements.

Description of $CaODA\cdot 6H_2O$ Structure

The crystal structure of calcium oxydiacetate hexahydrate ($CaODA\cdot 6H_2O$) contains $CaODA\cdot 5H_2O$ complexes which have approximate C_s-m point symmetry and which lie in the crystal such that the approximate mirror plane is perpendicular to {010}. The complexes are linked together only by hydrogen bonding which involves the sixth water molecule. Figure 1 illustrates

Table III. Interatomic Distances and Angles and Their Standard Deviations for $Ca[O(CH_2CO_2)_2]\cdot 6H_2O$[a]

A. Calcium Coordination			
Ca···O1	2.431 (3)	Ca···O8	2.497 (3)
Ca···O2	2.446 (3)	Ca···O9	2.549 (3)
Ca···O5	2.472 (3)	Ca···O10	2.422 (3)
Ca···O7	2.375 (2)	Ca···O11	2.455 (3)
B. Bonding Distances for Ligands			
O1–C2	1.447 (7)	O6–H15	1.15
O1–C3	1.403 (5)	O6–H16	1.15
C1–C2	1.505 (6)	O7–H9	0.95
C3–C4	1.513 (5)	O7–H10	0.92
C1–O4	1.250 (6)	O8–H11	0.91
C1–O5	1.267 (5)	O8–H12	0.88
C4–O2	1.254 (5)	O9–H13	0.75
C4–O3	1.268 (6)	O9–H14	0.89
C2–H1	1.05	O10–H5	1.01
C2–H2	0.94	O10–H6	0.84
C3–H3	0.94	O11–H7	0.87
C3–H4	1.11	O11–H8	0.96
C. Bond Angles for Ligands			
C2–O1–C3	112.4 (3)	O1–C3–H3	128
C1–C2–O1	109.2 (3)	O1–C3–H4	98
C4–C3–O1	109.0 (3)	C4–C3–H3	103
C2–C1–O4	116.3 (3)	C4–C3–H4	109
C2–C1–O5	118.2 (3)	H15–O6–H16	76
O4–C1–O5	125.5 (3)	H10–O7–H9	120
C3–C4–O2	119.7 (3)	H11–O8–H12	92
C3–C4–O3	114.3 (3)	H13–O9–H14	111
O2–C4–O3	126.0 (4)		
C1–C2–H1	102	H5–O10–H6	104
C1–C2–H2	119	H7–O11–H8	103
O1–C2–H1	111		
O1–C2–H2	103		
D. Hydrogen Bond Distances and Angles[b]			
O2···O9′	3.043 (4)	O5···O10′	2.809 (4)
O2···H14′	2.15	O5···H6′	2.00
O2···H14′–O9′	177	O5···H6′–O10′	163
O3···O6	2.928 (4)	O5···O7″	2.802 (3)
O3···H15	1.86	O5···H10″	1.99
O3···H15–O6	153	O5···H10″–O7″	147
O3···O7′	2.843 (8)	O6···O11′	2.976 (4)
O3···H9′	1.96	O6···H7′	2.11
O3···H9′–O7′	153	O6···H7′–O11′	174
O3···O8′	2.729 (4)	O6···O11″	2.865 (4)
O3···H12′	1.88	O6···H8″	1.95
O3···H12′–O8′	159	O6···H8″–O11″	160
O4···O8″	2.675 (4)	O8···O10″	2.834 (4)
O4···H11″	1.80	O8···H5″	1.85
O4···H11″–O8″	161	O8···H5″–O10″	164
O4···O9″	2.788 (4)	O9···O6′	3.006 (4)
O4···H13″	2.07	O9···H16′	1.96
O4···H13″–O9″	160	O9···H16′–O6′	150
E. Some Nonbonding Distances			
O2···O3	2.246 (3)	O1···O5	2.592 (3)
O4···O5	2.238 (4)	O1···O2	2.602 (4)

[a] Distances are in Ångströms and angles in degrees; standard deviations, where available, of the last significant figure are given in parentheses. [b] Prime symbols indicate atom positions symmetry related to those in Table I, as follows: O9′, H14′ $(x, y, 1 - z)$; O10′, H6′, O8″, H11″ $(x, y, -1 + z)$; O7″, H10″ $(1 - x, 1 - y, z)$; O7′, H9′ $(1/2 - x, 1 1/2 + y, -z)$; O8′, H12′, O9″, H13″ $(-1/2 + x, 1/2 - y, z)$; O11′, H7′ $(1/2 - x, 1 1/2 + y, 1 - z)$; O11″, H8″ $(1/2 + x, 1/2 - y, 1 + z)$; O10″, H5″ $(1 - x, 1 - y, 1 - z)$; O6′, H16′ $(1/2 - x, 1/2 + y, -z)$.

the packing of the molecules in the unit cell. Unlike the crystal structures of many calcium complexes, there is no Ca^{2+} bridging between ligands in this crystal lattice. All hydrogen bond lengths (Table III, range of OH···O distances is 2.675–3.043 Å) lie within the expected range of values. The hydrogen bond network is extensive; all carboxylate and water oxygens are involved in at least one or, more often, two or three hydrogen bonds.

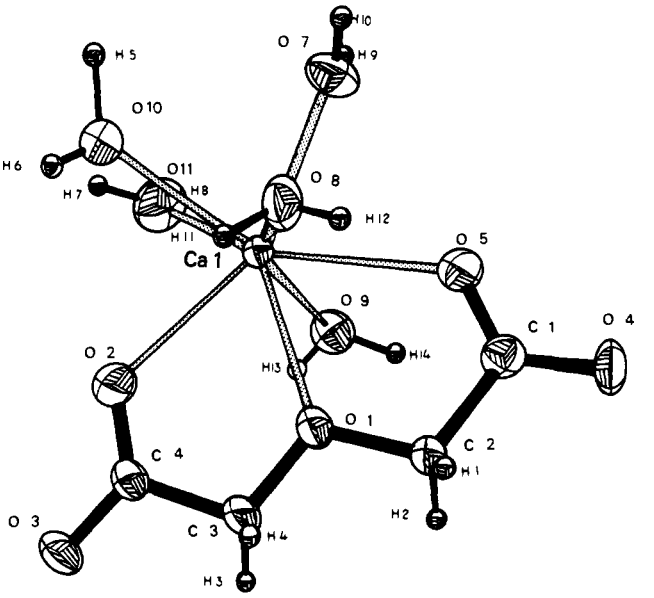

Figure 2. $CaODA\cdot 5H_2O$ complex.

Within the $CaODA\cdot 5H_2O$ complex (Figure 2) the CaODA moiety and one water molecule lie in an approximate mirror plane. The maximum deviation from planarity (Table IV) of the nonhydrogen atoms of the CaODA moiety is less than 0.1 Å, and one coordinated water molecule is displaced only 0.18 Å from this plane. The additional four coordinated water molecules are nearly equally disposed in pairs on either side of the $CaODA\cdot H_2O$ plane. The primary coordination sphere of the Ca^{2+} ion contains eight oxygen atoms, with Ca···O distances ranging from 2.375 to 2.549 Å; all other Ca···O distances are greater than 3.2 Å. The observed irregular eightfold coordination geometry is not unusual for Ca^{2+} complexes, particularly those containing multidentate chelating ligands. For example, $Ca_2EDTA\cdot 7H_2O$ also contains an eight-coordinate $CaEDTA^{2-}$ complex of irregular geometry; Ca···O distances are similar to those reported here.[14] Of the eight oxygen atoms bound to Ca^{2+} in $CaODA\cdot 5H_2O$, five are from water molecules and three are from the tridentate oxydiacetate ligand. That the ether oxygen of this ligand plays an important part in the Ca^{2+} coordination is shown by a short calcium–ether oxygen separation of 2.431 Å, compared to the slightly longer calcium–carboxylate oxygen separations, 2.472 and 2.446 Å. Although several examples of Ca^{2+} binding with donor atoms of neutral functional groups such as hydroxyl, carbonyl, and amine have been reported, to our knowledge only one other X-ray structural study of Ca^{2+} binding by an ether oxygen has appeared; this involves the Ca^{2+} complex of 5-keto-D-gluconate, in which the Ca^{2+} ion is bound, in part, by the lactol ring oxygen.[15,16]

(14) V. A. Uchtman, Abstracts, 162nd National Meeting of the American Chemical Society, Washington, D. C., Sept. 12–17, 1971, No. INORG 058. Manuscript in preparation.

(15) A. A. Balchin and C. H. Carlisle, *Acta Crystallogr.*, **19**, 103 (1965).

(16) A brief report on the crystal structure of calcium 4*H*-pyran-2,6-dicarboxylate trihydrate has appeared: K. J. Palmer and K. S. Lee, *Acta Crystallogr., Sect. B*, **25**, 2412 (1969). The material was found to be isomorphous with calcium dipicolinate trihydrate;[19] however, a detailed structural analysis was not reported.

Table IV. Equation of Least-Squares Planes and Distances (Å) from These Planes[a]

A. Plane Containing O1, O2, O3, O4, O5, C1, C2, C3, and C4			
$-0.4942X - 0.1185Y - 0.8612Z + 3.1232 = 0$			
O1	−0.018	C1	0.007
O2	−0.082	C2	−0.076
O3	0.061	C3	0.040
O4	−0.033	C4	0.004
O5	0.068		
		Ca	0.017
B. Plane Containing Ca, O1, O2, O3, O4, O5, C1, C2, and C4			
$-0.4922X - 0.1247Y - 0.8615Z + 3.1363 = 0$			
Ca1	0.001	C1	0.006
O1	−0.018	C2	−0.071
O2	−0.092	C3	0.045
O3	0.063	C4	0.003
O4	−0.031		
O5	0.059	O7	−0.185
C. Plane Containing Ca, O1, O2, O3, O4, O5, O7, C1, C2, C3, and C4			
$-0.4920X - 0.1103Y - 0.8636Z + 3.0661 = 0$			
Ca	0.018	C2	−0.091
O1	−0.034	C3	0.012
O2	−0.100	C4	−0.024
O3	0.023		
O4	−0.034	O8	−2.373
O5	0.074	O9	2.467
O7	−0.135	O10	−1.362
C1	0.005	O11	1.451
D. Plane Containing O4, O5, C1, and C2			
$-0.4815X - 0.1796Y - 0.8579Z + 3.3251 = 0$			
O4	−0.003	C1	0.013
O5	−0.002	C2	−0.004
E. Plane Containing O2, O3, C3, and C4			
$-0.4988X - 0.0512Y - 0.8652Z + 2.9219 = 0$			
O2	−0.000	C3	−0.001
O3	−0.000	C4	0.002
F. Plane Containing Ca, O1, O2, and O5			
$-0.5163X - 0.1441Y - 0.8442Z + 3.3447 = 0$			
Ca	0.001	O2	−0.007
O1	0.006	O5	−0.005

[a] The Smith least-squares plane program [D. L. Smith, Ph.D. Thesis (Appendix), University of Wisconsin (Madison), 1962] was utilized to obtain the equations of best planes formed by atoms indicated and also the perpendicular distances of these and other atoms from the planes. The equation of the least-squares plane is expressed in orthogonal coordinates X, Y, Z, which are related to cell coordinates by the transformation: $X = ax + b(\cos\gamma)y + c(\cos\beta)z$; $Y = [b(1 - \cos^2\gamma)^{1/2}]y + [c(\cos\alpha - \cos\beta\cos\gamma)/(1 - \cos^2\gamma)^{1/2}]z$; $Z = c[1 - \cos^2\beta - (\cos\alpha - \cos\beta\cos\gamma)^2/\sin^2\gamma]^{1/2}z$.

In the planar configuration of the oxydiacetate ligand the three donor oxygen atoms are ideally placed for tridentate binding to Ca^{2+}, as is demonstrated by the near equality of the three Ca···O distances. Tridentate chelation, as in CaODA, has also been found in the following calcium complexes:[17] calcium arabonate pentahydrate (calcium bound to oxygens from one carboxylate and two hydroxyl groups),[18] calcium dipicolinate trihydrate (oxygens from two carboxylates and a nitrogen from the pyridine ring),[19] calcium 5-keto-D-gluconate dihydrate (oxygens from a carboxylate, a hydroxyl, and a lactol ring),[15] and calcium malate dihydrate (oxygens from two carboxylates and a hydroxyl).[20]

In the present crystal structure, the oxydiacetate ligand exists with all nonhydrogen atoms nearly coplanar (Table IV). The interatomic bond distances and angles (Table III) are all within the ranges of expected and previously observed values. The ligand geometry is also not significantly different from that previously observed in the neodymium and ytterbium complexes of oxydiacetate,[21] where similar tridentate coordination is found.

Raman Results

Since the vibrational spectra of aqueous oxydiacetate and the parent acid have not, to our knowledge, been discussed previously in the literature, we present here Raman spectral data and proposed frequency assignments for this system. Our intention is to emphasize those spectral features which enter into the subsequent discussion of solution structures, rather than to give an exhaustive vibrational analysis.

In Table V are presented Raman frequencies and their

Table V. Raman Frequencies (cm^{-1}) and Assignments for Aqueous Sodium and Calcium Oxydiacetate and Solid $CaODA \cdot 6H_2O$[a]

1.0 *M* Na_2ODA	0.18 *M* CaODA[b]	CaODA·$6H_2O$(s)[c]	Assignment
2955 m, dp		2946 vs	Asym CH_2 str
2927 s, p		2921 vs	Sym CH_2 str
2890 m, p		2909 vs	Overtone or combination
~2863 sh, w, p		2863 w	
		2820 w	
	1720 w, p		Acid C=O str
~1597 sh, w, dp	~1605 m, dp	~1586 b, vw	COO^- asym str
1465 sh, w, p?	1465 mw, dp	1469 mw	CH_2 def
1449 mw, p			CH_2 def
	1439 s, p	1439 vs	COO^- sym str
1432 s, p	1421 m, dp	1420 mw	CH_2 def
1412 vs, p			COO^- sym str
1346 m, p	1357 m, p	1354 s	
~1323 b, w, dp			CH_2 wag
~1310 b, vw	1312 w, dp	1317 mw	
~1272 vw, dp	~1280 vw	1257 w	CH_2 twist
1245 mw, dp	1234 m, dp	1243 m	
1129 w, dp	~1135 b, w	1134 vw	COC asym str
1052 mw, p	1055 m, p	1066 m	COC sym str
987 vw, dp			CH_2 rock
952 m, p	953 vs, p	962 vs	
933 m, p			C–C str
916 vs, p			
	912 w, p		Acid C–C str
	887 m, p		
~713 b, w			
593 mw, dp			
~550 b, w, dp			Skeletal def
467 m, dp		473 mw	
~352 b, mw, p		356 m	

[a] Spectra were examined down to 300 cm^{-1}. For the complex contours near 950 and 1450 cm^{-1}, the data refer to resolved components. Abbreviations: s, strong; m, medium; w, weak; v, very; sh, shoulder; b, broad; p, polarized; dp, depolarized. [b] Solution contains 0.18 *M* Ca^{2+} and 0.18 *M* H_2ODA, three-fourths neutralized. Frequencies of bands at 1605 and 1720 cm^{-1} were obtained from a D_2O solution. The spectral regions above 2800 cm^{-1} and below 800 cm^{-1} are very weak and superimposed on steep backgrounds. [c] Bands observed at 535, 575, and 800 cm^{-1} are not listed, as they are instrumental artifacts which we usually encounter with solid samples.

(17) Multidentate chelation is common for Ca^{2+} complexation; examples of bi-, tri-, tetra-, and hexadentate binding and chelate rings of four, five, and six atoms have been reported in the literature.

(18) S. Furberg and S. Helland, *Acta Chem. Scand.*, **16**, 2373 (1962).

(19) G. Strahs and R. E. Dickerson, *Acta Crystallogr., Sect. B*, **24**, 571 (1968).

(20) C.-I. Brändin and B.-O. Söderberg, *Acta Chem. Scand.*, 20, 730 (1966).

(21) J. Albertsson, *ibid.*, **24**, 3527 (1970).

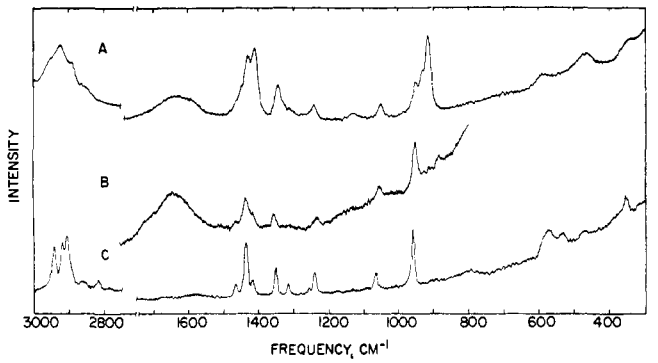

Figure 3. Laser-Raman spectra of (A) 1.0 M Na_2ODA, (B) 0.18 M Ca^{2+}–ODA (three-fourths neutralized), and (C) $CaODA \cdot 6H_2O$ solid. In A and B, the broad band at *ca.* 1640 cm^{-1} arises from the solvent. For further comments, see Table V, footnotes *b* and *c*.

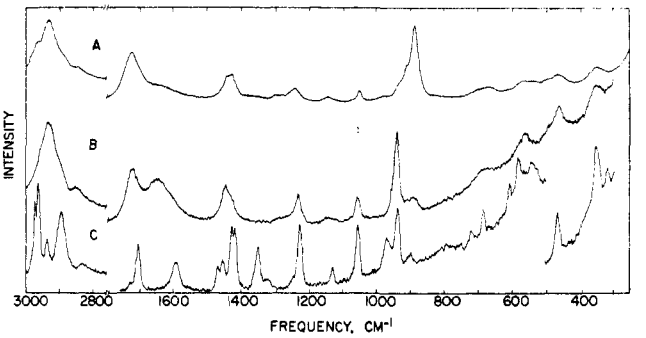

Figure 4. Laser-Raman spectra of (A) 3.0 M H_2ODA, (B) 1.0 M H_2ODA + 3.0 M $CaCl_2$, and (C) $Ca(HODA)_2$ solid. In A and B, the broad band at *ca.* 1640 cm^{-1} arises from the solvent. In C, there is some contribution from instrumental artifacts at 535, 575, and 800 cm^{-1}.

assignment for aqueous oxydiacetate solutions in the absence and presence of added equimolar Ca^{2+}, and for solid $CaODA \cdot 6H_2O$. The corresponding Raman spectra appear in Figure 3. The spectrum of aqueous Na_2ODA (Figure 3A) is representative of those obtained for ODA solutions not containing a strongly coordinating metal ion. However, even in the case of alkali metal ODA solutions, several spectral properties (systematically) depend to some extent on the identity of the cation.[22] The 1:1 Ca^{2+}–ODA solution which we examined was fairly dilute (0.18 M) and was prepared by *ca.* three-fourths neutralizing H_2ODA in the presence of equimolar $CaCl_2$. Solubility limitations of this solution ruled out the likelihood of appreciably increasing either its concentration or pH. However, its spectrum (Figure 3B) indicates only a small fraction of protonated carboxyl groups and is considered to be largely characteristic of Ca^{2+}–ODA complexation in aqueous solution (*vide infra*). Stability constant measurements lead us to infer that the most important complex in this solution is CaODA(aq) ($\log K_1 = 3.4$ at 30°).[4]

As an aid in interpreting the foregoing spectra of oxydiacetate in various environments, Raman frequencies and their assignment for aqueous 1.0 M H_2ODA are tabulated in Table VI. Included in this table are the corresponding data for a 1.0 M H_2ODA solution containing a threefold excess of Ca^{2+}, thus allowing assessment of possible interactions between Ca^{2+} and *un-ionized* H_2ODA. Figure 4 displays Raman spectra for 3.0 M H_2ODA (generally the same as that for 1.0 M H_2ODA, but with a greater signal-to-noise ratio), for a mixture of 1.0 M H_2ODA and 3.0 M $CaCl_2$, and for the solid which crystallizes from concentrated aqueous solutions which contain both H_2ODA and Ca^{2+}. This solid was identified by both elemental analysis and vibrational spectroscopy as anhydrous $Ca(HODA)_2$ (see Experimental Section); its complete frequency listing is not included here, as this information is not essential to the later discussion.

The Raman band assignments in Tables V and VI are based primarily on considerations of (1) well-documented group vibrational frequencies, (2) a comparison of spectra of H_2ODA and its dianion ODA, and (3) spectra of structurally related molecules, such as diethyl ether[23] and the glycolic (hydroxyacetic) acid–glycolate pair.[24] Except for COC modes, the vibrations of the molecules of interest can be viewed as in-phase and out-of-phase pairs resulting from coupling between motions of the two $CH_2COO(H)$ groups. The spectra reflect the extent of this coupling for the individual vibrations. For example, multiple bands assigned to the CH_2 deformation, wag, and twist modes are indicative of vibrational interaction between the two CH_2 groups.[13]

Special attention will be given to the C–C and C–O skeletal stretching vibrations of ODA and H_2ODA, located between 850 and 1150 cm^{-1}, as they are central to the discussion of solution structures to follow. Spectral comparison with related molecules is especially valuable here. For the aqueous glycolic acid–glycolate system,[24] a weak, slightly polarized line attributable primarily to alcoholic C–O stretching was seen at 1090

Table VI. Raman Frequencies (cm^{-1}) and Assignments for Aqueous Solutions Containing H_2ODA[a]

1.0 M H_2ODA	1.0 M H_2ODA + 3.0 M $CaCl_2$	Assignment
2970 ms, dp	~2960 sh, m, dp	Asym CH_2 str
2935 s, p	2933 vs, p	Sym CH_2 str
~2890 sh, w, p	~2898 sh, m, p	Overtone or combination
~2845 b, w, p	2847 mw, p	
1732 s, p	1727 s, p	C=O str
1448 ms, dp	1449 ms, dp	CH_2 def
1432 ms, dp	1431 sh, m, dp	
~1365 b, vw	1340 vw	CH_2 wag
1303 w		COH str, def
1284 w, dp	1284 vw, dp	CH_2 twist
	1251 sh, vw, dp	
1246 m, dp	1235 m, dp	
1146 mw, dp	1148 w, dp	COC asym str
1053 m, p	1059 m, p	COC sym str
978 w, dp		CH_2 rock
935 sh, m, p	943 vs, p	C–C str
913 sh, ms, p	~915 sh, vw, p	
889 vs, p	890 mw, p	
683[b] b, mw	~682 b, mw, p	Skeletal def
565 m, dp	560 mw, dp	
~535 sh, w, dp		
~490 b, sh, w		
466 m, p	461 m, dp	
353 m, p	349 m, p	

[a] See Table V, footnote *a*. [b] For 3.0 M H_2ODA, this band is seen to be a doublet with maxima at 671 and 705 cm^{-1}.

(22) R. P. Oertel, manuscript in preparation.

(23) H. Wieser, W. G. Laidlaw, P. J. Krueger, and H. Fuhrer, *Spectrochim. Acta*, **24**, 1055 (1968).

(24) Unreported results from this laboratory.

cm^{-1} for the acid and 1075 cm^{-1} for the salt. Tables V and VI list bands on either side of these positions for ODA and H_2ODA. Based on depolarization ratios and relative intensities, the lower frequency peak is best ascribed to symmetric COC stretching and the higher frequency peak to antisymmetric COC stretching. Comparable frequencies have been calculated and observed for vibrations involving COC stretching in diethyl ether and its deuterated analogs.[23] Considering again the glycolic acid–glycolate reference system, we observed a strong, highly polarized band at 890 cm^{-1} (acid) and 918 cm^{-1} (salt) which must be due mainly to C–C stretching. Prominent peaks occur at practically the same frequencies for aqueous H_2ODA (889 cm^{-1}) and Na_2ODA (916 cm^{-1}) and are similarly assigned.

We propose that the two polarized, higher frequency shoulders on each of these major C–C stretching bands (889 cm^{-1} for H_2ODA, 916 cm^{-1} for Na_2ODA) arise from stretching vibrations of C–C bonds in different chemical environments, *i.e.*, in various rotational isomers (*vide infra*). These shoulders appear not to be simply the result of vibrational interactions between C–C bonds within the same molecule. To be sure, some coupling exists between C–C and C–O bond-stretching motions, as evidenced by the simultaneous movement upon acid ionization of the COC antisymmetric stretching band (*ca.* 1135 cm^{-1}) and the entire spectral envelope assigned to C–C stretching. Such interaction must not be great, because when H_2ODA is dissolved in D_2O the C–C multiplet shifts downward from 889/913/935 to 852/880/908 cm^{-1}, whereas both COC stretching bands exhibit only minor (*ca.* 4 cm^{-1}) upward shifts.[25] Since interaction between C–C and C–O stretching apparently is weak, we anticipate that coupling between the two C–C bonds is even less important. A demonstration of this was seen in the Raman spectrum of an aqueous solution containing half-neutralized H_2ODA (0.33 *M* NaHODA). Here, the spectral contour in the C–C stretching region approximated a superposition of C–C stretching multiplets (*ca.* equally weighted) observed for 1.0 *M* H_2ODA and 1.0 *M* Na_2ODA alone, suggesting that the two C–C bonds are vibrating virtually independently of one another. Furthermore, for certain ODA-containing samples this spectral region can contain only a *single* band attributable to independent stretching of *two* C–C bonds. This is seen most clearly in the spectrum of solid $CaODA \cdot 6H_2O$ (Figure 3C).

On the basis of the frequency assignments, several additional facts should be pointed out concerning the spectra in Figures 3 and 4. First, in the spectrum of CaODA(aq) (Figure 3B), the low intensity of bands at 887, 912, and 1720 cm^{-1} indicates only a low level of un-ionized COOH groups. Moreover, when this solution is prepared in D_2O, the strong 953-cm^{-1} band is not shifted to lower frequency, a fact which shows that this band is due predominantly to CaODA(aq) and not to a species containing COOH groups.[25] Second, the weakness or absence of polarized peaks at *ca.* 1350 and *ca.* 1425 cm^{-1} in Figures 4A and 4B rules out the presence of all but small amounts of CH_2COO^- groups in these concentrated acid solutions.[26] Third, the appearance of prominent lines at both 1593 and 1709 cm^{-1} in Figure 4C is in accord with the composition $Ca(HODA)_2$, containing both ionized and un-ionized acid groups.

(25) Deuteration of the acidic proton leads to a lowering of C–C stretching frequencies presumably owing to mixing between C–C and C–OH vibrations.

Discussion

Structure of CaODA(aq). Combined with the X-ray structure determination of $CaODA \cdot 6H_2O$, the present Raman spectroscopic study provides an illuminating structural comparison between the CaODA complex in the solid state and in aqueous solution. Ultimately, one would like to relate the information so obtained regarding the essential characteristics of the CaODA-(aq) structure to important Ca^{2+}-dependent solution processes such as those involving biological Ca^{2+} transport and utilization.

As was suggested earlier and will be amplified below, Raman spectra of the aqueous H_2ODA–ODA system are explained most satisfactorily by postulating the existence of rotational isomers in these solutions. Raman spectra characteristically are quite sensitive to changes in the relative disposition of skeletal atoms in a molecule. The spectrum of the ODA ligand, for example, is expected to reflect changes in the CCOCC backbone conformation. By comparison with related five-atom molecular skeletons, *e.g.*, diethyl ether[23] and *n*-pentane,[27] the following three spectroscopically distinguishable backbone geometries are regarded as most likely for ODA (illustrated below): trans–trans (TT), trans–gauche (TG), and gauche–gauche (GG).[28] For liquid *n*-pentane and diethyl ether the TT form predominates, in coexistence with a smaller amount of the TG form. In the case of H_2ODA and ODA, space-filling molecular models for all three geometries can be constructed relatively free of steric restraints. For such a complex system involving extensive hydrogen bonding with the solvent and ion–ion charge repulsion (in ODA), it does not appear possible to predict *a priori* the relative stabilities of these isomeric forms.

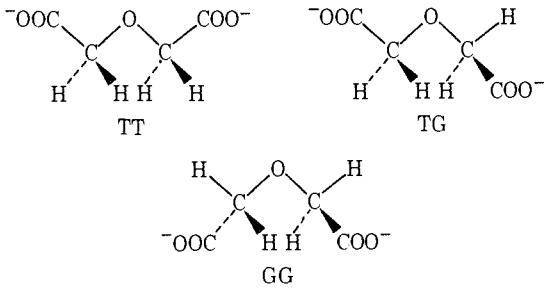

However, results of the X-ray analysis of $CaODA \cdot 6H_2O$ lead to the conclusion that the Raman spectrum of this solid (Figure 3C) is the spectrum of the ODA ligand entirely in its TT form. Subsequently, the remarkable likeness between Raman spectra of this solid and the CaODA(aq) solution complex (Figure 3B) convincingly establishes the identity of ODA skeletal

(26) Infrared spectra of similar solutions (in D_2O) do reveal an antisymmetric COO^- stretching peak at *ca.* 1600 cm^{-1}, though this is substantially weaker than the band due to acid carboxyl stretching at *ca.* 1725 cm^{-1}.

(27) S. Mizushima, "Structure of Molecules and Internal Rotation," Academic Press, New York, N. Y., 1954, pp 98–103.

(28) In this report we use the term "trans" in the conformational sense; elsewhere the synonymous term "anti" may be used. See, *e.g.*, E. L. Eliel, "Stereochemistry of Carbon Compounds," McGraw-Hill, New York, N. Y., 1962, p 126.

conformations (TT) in both of these complexed states. One is drawn to this conclusion all the more naturally in view of the extensive changes induced by the addition of Ca^{2+} to an ODA solution (compare Figures 3A and 3B). This is particularly evident in the 900–1000- and 1400–1500-cm^{-1} regions, where the introduction of Ca^{2+} reduces complex spectral patterns to simpler ones which, as noted above, are the same as those observed for solid $CaODA \cdot 6H_2O$. It is this spectral simplification which is especially reminiscent of the behavior of systems composed of rotational isomers; quite often for such systems, for example, a complicated room temperature Raman spectrum (representing several conformers) is converted into the spectrum of only a single form when the sample is frozen.[27] Many of the actual frequencies in the two CaODA spectra agree very closely, but the comparison is by no means perfect. Exact correspondence in frequency between solution and solid phases is not necessarily to be expected, however, owing to possible solid-state constraints and solvation perturbations. Any frequency differences (noted in Table V) between the two CaODA species probably can be attributed to such environmental influences.

Since the COO^- groups of ODA are too greatly separated to interact vibrationally,[29] it is difficult to determine from the spectral data their relative orientation in solution. We can account for concurrent frequency shifts of both the COO^- symmetric stretching and C–C stretching bands when Ca^{2+} is added to an ODA solution by recognizing that these modes can and probably do couple to some extent.[30] Having learned that Ca^{2+} promotes the adoption of the planar (TT) ODA backbone in aqueous solution, we are inclined to believe that for maximization of Ca–O coulombic interactions in CaODA(aq) the COO^- groups must be coplanar with each other and also with the CCOCC backbone plane. An implicit assumption here is that, as in solid $CaODA \cdot 6H_2O$, CaODA(aq) must possess two adjacent five-membered chelate rings containing Ca^{2+} and the ether oxygen atom. Such chelation is implied, however, by the comparatively high value of the measured 1:1 stability constant, $\log K_1 = 3.4$.[4] This value may be compared with the lower values of $\log K = 0.50$ for the 1:1 Ca^{2+}–acetate complex[31] and $\log K = 1.59$ for the 1:1 Ca^{2+}–glycolate complex.[32] The last value is *ca.* half that of the CaODA(aq) stability constant, in accord with the notion that the glycolate complex contains one, and the ODA complex two, five-membered chelate rings. If, as may be reasonably assumed, the two lone electron pairs in the valence shell of the ODA ether oxygen occupy sp^3-like orbitals, then in the CaODA planar structure the Ca^{2+}–ether oxygen bond vector bisects the angle made by these lone electron pairs. This arrangement suggests that *both* lone electron pairs play a significant and equal role in the attraction between the Ca^{2+} and the ether oxygen.

The interaction between Ca^{2+} and the carboxylate oxygen atoms is primarily ionic, as shown by the small perturbation (a frequency increase of only *ca.* 8 cm^{-1}) of the broad, antisymmetric COO^- stretching band when Ca^{2+} binds ODA in solution. An unsymmetrical metal–carboxylate coordination geometry, as in the present case, should lead to a larger frequency increment for this band if significant metal–oxygen covalency were involved.[33] The near equivalence of the four carboxylate C–O distances in solid $CaODA \cdot 6H_2O$ (range 1.250–1.268 Å) is in accord with this simple electrostatic description of Ca–O bonding.

Therefore, we feel that the majority of Raman spectral changes observed when Ca^{2+} binds ODA in solution arise not from changes in force constants induced directly by Ca^{2+}, but rather from differences in vibrational coupling accompanying conformational interconversion to the TT form. This is expected to be especially valid for bands which result from coupled vibrations of the two CH_2 groups. In addition, the dramatic dependence on molecular geometry of the C–C stretching frequency is reasonably attributed to coupling of this mode (though apparently only weakly, *vide supra*) with the COC vibrations.

Possible Conformers of ODA in the Na_2ODA Solution. Several Raman bands observed for the TT isomer in CaODA(aq) might be predicted also to contribute to a spectrum of the ODA anion in its TG form, *i.e.*, some peaks might be characteristic of the trans geometry of either half of the dianion. Among these are the 953- and 1439-cm^{-1} lines, both originating from vibrations mainly localized in only half of the dianion. Therefore, observation of such bands in the Na_2ODA spectrum does not necessarily indicate the presence of the TT form in this solution.

Bearing this in mind, we note a medium-intensity 952-cm^{-1} band in Figure 3A very close to the observed C–C stretching frequency for the CaODA(aq) complex. The strong, polarized symmetric COO^- stretching band also seen for the TT isomer might then be expected to lie near 1439 cm^{-1} in the Na_2ODA spectrum and exert a noticeable effect on the spectral envelope in that region. Indeed, its underlying presence is suggested by (1) the high intensity ratio of the resolved component at 1432 cm^{-1} to that at 1449 cm^{-1}, compared with the aqueous H_2ODA spectrum where these CH_2 deformation bands are equally intense and (2) the observation that the resolved components at 1432 and 1449 cm^{-1} are polarized in the Na_2ODA spectrum but depolarized in the H_2ODA spectrum. In addition, the weak 1465-cm^{-1} shoulder in the Na_2ODA spectrum probably is associated with the trans geometry about the skeletal C–O bonds, since a similar peak is exhibited by the CaODA complex.

These Raman lines arising from the trans geometry (in TT and/or TG) are not the most intense in the Na_2ODA spectrum; the dominating bands probably are due to gauche moieties in the TG and GG isomers. Molecular models indicate that the TG and GG rotational isomers of ODA might well be stabilized to some extent by C–H···$^-$OOC hydrogen bonding,[34] in the absence of any overriding influence such as Ca^{2+}. On the basis of the available data, little more can be said to provide a clearer description of structure in the Na_2ODA solution.

(29) C. B. Baddiel, C. D. Cavendish, and W. O. George, *J. Mol. Struct.*, **5**, 263 (1970).
(30) E. Spinner, *J. Chem. Soc.*, 4217 (1964).
(31) J. W. Bunting and K. M. Thong, *Can. J. Chem.*, **48**, 1654 (1970).
(32) C. W. Davies, *J. Chem. Soc.*, 277 (1938).
(33) D. T. Sawyer and P. J. Paulsen, *J. Amer. Chem. Soc.*, **80**, 1597 (1958).
(34) D. J. Sutor, *J. Chem. Soc.*, 1105 (1963).

Implications of TT Ligand Geometry in CaODA. With respect to the chelating OCCOCCO chain of atoms, the ODA ligand in the CaODA complex has a close structural similarity to analogous metal chelating fragments in cyclic polyether molecules, *e.g.*, "dibenzo-18-crown-6" (as structurally characterized in the rubidium sodium isothiocyanate complex[35]) and in certain macrocyclic antibiotics, *e.g.*, monensin (as structurally characterized in the silver ion complex[36]). This resemblance suggests that oxydiacetate may have biological activity, particularly with respect to membrane transport of metal ions. Recent evidence has been accumulated[37] which, in fact, indicates an unusually high percutaneous toxicity for aqueous sodium oxydiacetate. The only major structural differences in the chelating fragments (as shown above) of these molecules are the following. The O–C–C (carbonyl) angles are close to a trigonal value of 120° in ODA, while in the cyclic polyether and macrocyclic antibiotic these angles are close to a tetrahedral value of 109°. Also, as noted previously, the OCCOCCO fragment is planar in CaODA while in the other molecules considerable deviations from planarity exist. It should be possible to utilize the structural characteristics of the CaODA complex to postulate (cyclic) molecules which could be selective for Ca^{2+} and have the ability to "carry" or "shuttle" Ca^{2+} in biological systems.

Ca^{2+}–H_2ODA Complexation. Cyclic Ca^{2+} chelates such as suggested above might well involve binding between Ca^{2+} and formally uncharged ligands. In an attempt to find evidence of Ca^{2+} binding to neutral H_2ODA, we carried out Raman studies on pH-unadjusted solutions containing Ca^{2+} and H_2ODA. The obvious similarity in appearance of the C–C stretching multiplet in Raman spectra of aqueous H_2ODA (Figure 4A) and Na_2ODA (Figure 3A) suggests that generally the same type and population of rotational isomers exist in both solutions.[38] The striking spectral transformation resulting from addition of a calcium salt to the H_2ODA solution (Figure 4B) clearly is indicative of Ca^{2+} complexation, albeit much weaker than that between Ca^{2+} and ODA. That the spectral changes might simply be a general electrolyte perturbation of the water structure, which in turn alters the relative isomer population, is ruled out by the observation that 2.0 *M* LiCl has no effect on the Raman spectrum of 1.0 *M* H_2ODA.

As mentioned earlier, the spectra indicate only a minor amount, at most, of H_2ODA ionization even in the presence of 3.0 *M* $CaCl_2$. The predominant form of the ligand therefore must be fully protonated H_2ODA. To check this conclusion we prepared a solution containing 1 *M* H_2ODA, 3 *M* $CaCl_2$, and 1 *M* HCl and found no significant spectral variation compared with Figure 4B. If complexation were only between Ca^{2+} and, for example, HODA, addition of HCl should have had considerable effect on the spectrum.

Many bands, including those due to skeletal deformations and carboxyl stretching, become sharper in the presence of Ca^{2+}, suggesting fewer rotational isomeric possibilities for the H_2ODA ligand. In addition, the carboxyl stretching frequency shifts downward, probably due to direct Ca^{2+}–carboxyl interaction. A single polarized peak gains prominence at the high-frequency edge of the C–C stretching region of H_2ODA (943 cm^{-1}), behavior reminiscent of that caused by total conversion of ODA to the TT form in its Ca^{2+} complex. Based on the last observation we feel disposed toward postulating that the chelating H_2ODA ligand also possesses TT geometry. Some support for this is provided by the frequency shifts of the COC stretching and CH_2 twisting bands upon addition of Ca^{2+}; these shifts are in the same direction as seen when Ca^{2+} binds ODA in its TT form. On the other hand, a discrepancy exists in that the CH_2 deformation bands are *not* split as far apart upon Ca^{2+} complexation in H_2ODA solution as they are for CaODA(aq).

From quantitative measurement of the intensity (height) of the 890-cm^{-1} H_2ODA band, using the 1948-cm^{-1} line of added NO_3^- as an internal standard,[39] we were able to estimate the concentration formation quotient for the 1:1 Ca^{2+}–H_2ODA complex as $K = 0.56 \pm 0.15\ M^{-1}$ at *ca.* 30°. For this series of determinations the formal H_2ODA concentration was varied from 0.25 to 1.0 *M* and the stoichiometric ratio $[CaCl_2]/[H_2ODA]$ maintained at 3, thus favoring formation of the 1:1 H_2ODA:Ca^{2+} species (multinuclear calcium species initially were assumed insignificant and are shown to be so by the relative constancy of *K*). Possible complexes having higher H_2ODA/Ca^{2+} ratios were not investigated. The calculated equilibrium quotient is small, but nevertheless very real. It probably represents a lower limit of the actual value, since the NO_3^- standard is known to complex Ca^{2+} very weakly in aqueous solution[40] and thus will compete to a slight extent with H_2ODA for Ca^{2+} coordination sites. The fact that *K* is measurable at all probably rests on the fact that two five-membered chelate rings are formed by Ca^{2+}, the two neutral carboxyl oxygens, and the ether oxygen atom. We would expect, of course, greater stability for the complexes formed between Ca^{2+} and proposed cyclic ligands (*vide supra*) which have more chelating ability than H_2ODA.

Solid $Ca(HODA)_2$. We conclude by pointing out several salient features of the $Ca(HODA)_2$ solid which readily is produced in aqueous solutions containing a calcium salt and H_2ODA (pH not adjusted). Whereas $CaODA \cdot 6H_2O$ crystallizes from solutions containing a preponderance of the identical 1:1 aqueous complex, $Ca(HODA)_2$ forms from solutions in which Ca^{2+}–H_2ODA species dominate (compare Figures 4B and 4C). The formation of $Ca(HODA)_2$ does not depend greatly on the solution stoichiometry, and the solid appears even in solutions acidified with HCl. Its structure must represent an unusually stable arrangement. Moreover, the fact that it is anhydrous is exceedingly uncommon among Ca^{2+} complexes of chelating organic ligands;

(35) D. Bright and M. R. Truter, *J. Chem. Soc. B*, 1544 (1970).
(36) M. Pinkerton and L. K. Steinrauf, *J. Mol. Biol.*, **49**, 533 (1970).
(37) The Procter & Gamble Co., unpublished results.
(38) The reported ^1H nmr spectrum of H_2ODA in acetone-d_6 and DMSO-d_6 revealed only a single resonance at *ca.* τ 5.80 which was attributed either to a molecular geometry having a plane of symmetry passing through all heavy atoms or to rapid oscillation about such an average geometry: A. Solladie-Cavallo, *Bull. Soc. Chim. Fr.*, 437 (1968). We found a single resonance at τ 5.72 for 2.0 *M* H_2ODA in D_2O. The second interpretation is in better accord with the Raman results.
(39) In order to correct the NO_3^- 1048-cm^{-1} intensity for the contribution at 1055 cm^{-1} due to H_2ODA species, a height equal to that of the *ca.* 1240-cm^{-1} band was subtracted. The 1055- and 1240-cm^{-1} peaks are roughly equally intense in H_2ODA spectra.
(40) R. E. Hester and R. A. Plane, *J. Chem. Phys.*, 40, 411 (1964).

usually, as in crystalline $CaODA \cdot 6H_2O$, water molecules are included to satisfy the preferred coordination number of eight for Ca^{2+}.

The vibrational spectra of this material cannot unambiguously be interpreted at present to help elucidate its structure, except in one respect. The absence of a 1660-cm^{-1} Raman line rules out the formation of hydrogen bonded dimers between COOH groups of neighboring HODA ligands.[41] Because $Ca(HODA)_2$ very likely provides an illustration of Ca^{2+} binding to both neutral carboxyl and ether oxygen atoms, we are about to carry out the single-crystal X-ray determination of its expectedly interesting structure.[42]

Acknowledgments. The authors acknowledge the experimental assistance of M. Becker and K. Littlepage.

(41) Acid dimers are known to display the Raman-active carboxyl stretching vibration at *ca.* 1660 cm^{-1} [N. B. Colthup, L. H. Daly, and S. E. Wiberley, "Introduction to Infrared and Raman Spectroscopy," Academic Press, New York, N. Y., 1964, p 258] as we found for solid H_2ODA, for example.

(42) NOTE ADDED IN PROOF: We are grateful to Drs. S. H. Whitlow and G. Davey of the Department of Environment, Ottawa, Canada, for communicating to us their X-ray structure data for oxydiacetic acid prior to publication and for permitting us to mention them here. They have determined the acid skeletal conformation to be gauche–gauche in the solid state, in complete accord with the preceding spectral interpretation. During the course of our work, we observed C–C stretching bands only at 890 (vs) and 876 cm^{-1} (m) for this material (the latter probably due to vibrational coupling in the solid phase). Unlike the spectrum of aqueous H_2ODA, peaks located near the assigned frequency for the trans–trans acid conformer, *ca.* 940 cm^{-1}, were conspicuously absent (*cf.* Table VI and the section on Ca^{2+}–H_2ODA complexation).

Transition Metal Cyanocarbon Derivatives. I. Polycyanovinyl, Dicyanovinylidene, and Dicyanomethylene Derivatives of Metal Carbonyls from Cyanocarbon Halides and Metal Carbonyl Anions[1,2]

R. B. King* and Mohan Singh Saran[3]

Contribution from the Department of Chemistry, University of Georgia, Athens, Georgia 30601. *Received September 27, 1972*

Abstract: Reactions of the sodium salts $NaM(CO)_3C_5H_5$ (M = Mo and W), $NaMn(CO)_5$, and $NaFe(CO)_2C_5H_5$ with the 2,2-dicyanovinyl chlorides $(NC)_2C{=}C(X)Cl$ (X = H, CN, and Cl) in tetrahydrofuran solution give the corresponding polycyanovinyl transition metal derivatives $(NC)_2C{=}C(X)M(CO)_3C_5H_5$ (X = H, CN, and Cl; M = Mo and W), $(NC)_2C{=}C(X)Mn(CO)_5$ (X = H, CN, and Cl), and $(NC)_2C{=}CHFe(CO)_2C_5H_5$ in fair to good yields. Reaction of $NaFe(CO)_2C_5H_5$ with $(NC)_2C{=}CCl_2$ in tetrahydrofuran solution gives low to very low yields of the cis and trans isomers of $(C_5H_5)_2Fe_2(CO)_3[C{=}C(CN)_2]$, which are the first known transition metal complexes of the dicyanovinylidene (dicyanomethylenecarbene) ligand. Reaction of $NaFe(CO)_2C_5H_5$ with $(NC)_2CBr_2$ in tetrahydrofuran solution gives low yields of $(C_5H_5)_2Fe_2(CO)_3C(CN)_2$ containing a bridging dicyanomethylene group and of $(NC)_2CHFe(CO)_2C_5H_5$, the first dicyanomethyl transition metal derivative. The infrared and proton nmr spectra of these new compounds are discussed.

Within the last few years the reactions of metal carbonyl anions with various halogen compounds have been used to prepare a variety of unusual transition metal organometallic compounds.[4] This paper reports the extension of reactions of this type to the synthesis of novel cyanocarbon derivatives of transition metals by reactions of metal carbonyl anions with various cyanocarbon halides, particularly polycyanovinyl chlorides. New cyanocarbon derivatives described in this paper include not only a wide range of polycyanovinyl derivatives of molybdenum, tungsten, manganese, and iron but also the first known compounds with dicyanovinylidene (dicyanomethylenecarbene[5]) ligands bonded to transition metals.

(1) For a preliminary communication of this work, see R. B. King and M. S. Saran, *J. Amer. Chem. Soc.*, **94**, 1784 (1972).

(2) Portions of this work were presented at the 162nd National Meeting of the American Chemical Society, Washington, D. C., Sept. 1971, Abstract INOR 160.

(3) Postdoctoral research associate, 1969–1973.

(4) R. B. King, *Accounts Chem. Res.*, 3, 417 (1970).

(5) The name "dicyanovinylidene," for the carbene ligand $:C{=}C(CN)_2$, seems preferable to the longer name "dicyanomethylenecarbene," used in the preliminary communication (ref 1).

Experimental Section

Microanalyses were performed by Meade Microanalytical Laboratory, Amherst, Mass., and by Mr. M. L. Kshatriya and Mr. W Swanson of the Microanalytical Laboratory at the University of Georgia. Infrared spectra (Table I) were taken in dichloromethane solutions or potassium bromide pellets and recorded on a Perkin-Elmer Model 621 spectrometer with grating optics. Proton nmr spectra were taken in $CDCl_3$ solutions and recorded on a Varian HA-100 spectrometer at 100 MHz. Melting points were taken in capillaries and are uncorrected.

A nitrogen atmosphere was always provided for the following three operations: (a) carrying out reactions, (b) handling all filtered solutions of organometallic compounds, (c) filling evacuated vessels containing organometallic compounds. Alumina for chromatography (80–200 mesh) was used as received from Matheson Coleman and Bell.

Materials: Malononitrile and tetracyanoethylene were purchased from Kay-Fries Chemicals, Inc., New York, N. Y. Malononitrile was converted to 2,2-dicyanovinyl chloride ($(NC)_2C{=}CHCl$)[6] and this to 1,1-dichloro-2,2-dicyanoethylene[7] ($(NC)_2C{=}CCl_2$) by the cited published procedures. Tetracyanoethylene was converted to

(6) K. Friedrich, *Angew. Chem., Int. Ed. Engl.*, **6**, 959 (1967).

(7) A. D. Josey, C. L. Dickinson, K. C. Dewhirst, and B. C. McKusick, *J. Org. Chem.*, **32**, 1941 (1967).